PHILOSOPHICAL TRANSACTIONS OF THE ROYAL SOCIETY A MATHEMATICAL, PHYSICAL & ENGINEERING SCIENCES

Asymptotic theory of liquid–solid impact

A. A. Korobkin

Phil. Trans. R. Soc. Lond. A 1997 **355**, 507-522
doi: 10.1098/rsta.1997.0021

Asymptotic theory of liquid–solid impact

By A. A. Korobkin

Lavrentyev Institute of Hydrodynamics
Novosibirsk, 630090, Russia

The liquid–solid impact problem is analysed with the help of the method of matched asymptotic expansions. This method allows us to estimate the roles of different effects (viscosity of the liquid, surface tension, compressibility, nonlinearity, geometry) on the impact, to distinguish the regions of the flow and the stages of the impact, where and when each of these effects is of major significance, to present a complete picture of the flow, and describe approximately such phenomena as jetting, escape of the shock onto the liquid-free surface and cavitation. Five stages of the impact are distinguished: supersonic stage, transonic stage, subsonic stage, inertia stage and the stage of developed liquid flow. The asymptotic analysis of each stage is based on general principles of hydrodynamics and will be helpful to design experiments on liquid impact and to develop an adequate computational algorithm, as well as to understand the dynamics of the process.

1. Introduction

The phenomenon of liquid–solid impact is very complicated; it is accompanied by many effects, descriptions of which cannot be achieved in detail. All available theoretical models of the impact are limited in their validity. The limitations for numerical models are much stronger than for theoretical ones. Analytical models (theoretical models which allow their analytical investigation) are restricted by definition. This means that all we may expect from theoretical or numerical analysis is a 'sketch' (caricature) of the phenomenon and estimations of some characteristics. Those are mainly estimations of orders of quantities and effects in particular situations when some effects are of major significance but other ones can be disregarded. It is the standard case for obtaining the estimations when there are only two main effects and the process evolution is a realization of the balance between them.

Despite the great limitations of analytical models and analytical methods in their validity, they are powerful tools to study impact phenomena. The reason is that analytical models are able to predict directly the evolution of the process and its main peculiarities in detail but only in very specific situations. However, it frequently occurs that the total process can be described approximately with the help of a combination of such specific analytical models. This is the basis of the asymptotic methods which are very helpful in many problems of applied mathematics, mechanics and physics (see Van Dyke 1964).

Asymptotic theories are developed to analyse processes which deviate only a little from a main process. The description of the latter must be very simple. In the liquid impact problem with which we are concerned here, it is the rest state. Asymptotic

Phil. Trans. R. Soc. Lond. A (1997) **355**, 507–522
Printed in Great Britain

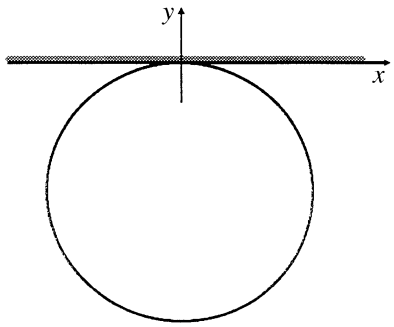

Figure 1. Impact by a flat plate on a circular liquid drop.

theory of impact is based on the general principles of hydrodynamics. Theoretical models of the liquid–solid impact include:

(1) assumptions about both the liquid and the solid properties and the interaction, as well as about the medium in which the liquid and solid masses are placed;

(2) equations of the liquid motion;

(3) boundary and initial conditions.

The model must be well posed, i.e. its solution must exist, be unique and weakly dependent on small variations of parameters, initial and boundary conditions. In many cases, this solution can be determined only numerically. Complete analysis of the theoretical model of liquid–solid impact is not available at present. That is why the connection of the present asymptotic theory with the theoretical model is only formal.

The asymptotic theory of liquid–solid impact is a collection of models which are simpler than the original one. The main part of them allow their analytical analysis and make it possible to present their solutions in analytical form. The models are connected with each other, but some of them can be analysed independently. This set of analytical models is referred to as the asymptotic theory because the models, together with links between them are self-consistent, include the main part of the approximate models of the impact derived before, give a truth-like description of the phenomena, correspond to the main part of experimental and numerical results, and clarify the direction of further investigations. This theory may be helpful to design experiments on liquid impact, to develop adequate computational algorithms, and to clarify our understanding of impact phenomena.

Both the shape of the liquid volume and the geometry of the rigid surface are of great importance and determine peculiarities of the impact process. In order to demonstrate the abilities of the asymptotic theory, a simple geometry of impact is considered here as being basic. Initially the liquid occupies a thin circular cylinder placed adjacent to a plate. The liquid boundary is free and touches the flat rigid surface at a single point (figure 1). This case corresponds to the experimental configuration discussed by Camus (1971) and Lesser & Field (1983*b*). The asymptotic theory is presented for the plane case but where it is possible, generalizations for three-dimensional case and for more complicated geometries of both the liquid and solid masses are given.

The general description of the events occurring during the impact is provided under the following assumptions: the liquid flow is planar; the impacting solid plate is undeformable; the impact velocity V is constant; the Mach number $M = V/c_0$,

where c_0 is the sound speed in the liquid at rest, is much less than unity; the effects of viscosity, surface tension and gravity are small compared with inertial effects.

The impact process can be divided into the following five stages: supersonic; transonic; subsonic; inertia and developed liquid flow. In the first four stages, the deformations of the liquid volume are small and can be approximately neglected outside small regions close to the periphery of the impact area. The hydrodynamic pressures at these stages are relatively large and decay with time. At the fifth stage the liquid flow is already developed and the deformations of the liquid volume have to be taken into account, however, the pressures are much lower than at the previous stages and cannot usually be classified as impact pressures. The focus of the present paper is on the first four stages.

For the ideal liquid model the velocities of the intersection points between the initial circular free surface and the flat solid surface are greater than the local sound speed for small times. This means that just after the impact moment the disturbed part of the liquid is bounded by the solid surface on one side and by a shock front on the others, the free surface therewith remains undisturbed (see Bowden & Field 1964). This stage is referred to as the supersonic stage. The duration of this stage is of order $O(M^2R/V)$, where R is the radius of the liquid volume, the dimension of the contact region is of order $O(RM)$ for small M. The quantity $T_1 = M^2R/V$ is taken in the present analysis to be the time scale, RM the length scale and V the scale of the liquid velocity. At this stage the liquid compressibility is of major significance. Viscous and capillary effects are localized in space and can be neglected in the leading order almost everywhere.

The next, transonic, stage starts when the velocities of the contact points approach the sound speed. At this stage the hydrodynamic pressure reaches its maximum and the deformation of the liquid surface has to be taken into account close to the contact points. This is the stage at which spray jets start to form, the speed of the contact region expansion drops below the sound speed, the shock front escapes onto the free surface and the jets are already developed at the end of the stage. The duration of this stage is much shorter than the supersonic stage.

At the subsonic stage the flow region can be divided into two main parts: the liquid bulk, where the deformations of the liquid boundary are small; and the jet region, which is attached to the solid surface.

At the inertia stage the shock wave is already far away from the contact region, and the compressibility effects are localized near the shock front. Behind the shock wave the flow can be treated as approximately incompressible.

The general description of the impact process given here is reasonable and understandable from a physical point of view, but in order to obtain more information about the flow and the pressure distribution, we need to derive analytical models for each stage.

2. Formulation of the problem

It is convenient to start from the general Navier–Stokes equations of liquid motion, which in dimensionless variables have the form

$$\rho(\boldsymbol{u}_t + M(\boldsymbol{u}\cdot\nabla)\boldsymbol{u}) = -\nabla p + Re^{-1}[\Delta\boldsymbol{u} + (\zeta/\eta + \tfrac{1}{3})\nabla(\nabla\cdot\boldsymbol{u})] - Fr^{-1}\,\rho\boldsymbol{e}_2, \qquad (2.1)$$

$$\rho_t + M(\nabla\cdot\rho\boldsymbol{u}) = 0, \qquad (2.2)$$

where $\boldsymbol{u} = (u, v)$ is the velocity vector, p is the pressure, ρ is the liquid density, η is the coefficient of viscosity, ζ is the second viscosity coefficient, $\boldsymbol{e}_2 = (0, 1)$, $Re = RV/\nu$ is the Reynolds number, ν is the kinematic viscosity coefficient, $Fr = c_0^2/gR$ is the Froude number and g is the acceleration due to gravity. The length, time and velocity scales were introduced in § 1. The initial liquid density ρ_0 is chosen as the density scale, and the 'water hammer' pressure $\rho_0 c_0 V$ as the pressure scale. The equation of state is in the Tate form and can be written as

$$\rho = (1 + nMp)^{1/n} \tag{2.3}$$

(where $n = 7.14$ for water). The point of the first contact between the liquid and the solid surface is taken as the origin of the Cartesian coordinate system Oxy, the axis Ox being directed along the rigid plate (see figure 1). On the free surface, the position of which is described by the equation $H(x, y, t) = 0$, the kinematic condition

$$H_t + M\boldsymbol{u} \cdot \nabla H = 0, \tag{2.4}$$

the condition of absence of tangential stresses,

$$\boldsymbol{n} \cdot \mathcal{R} \cdot \boldsymbol{t} = 0, \tag{2.5}$$

and the condition for the normal component of the stress vector,

$$\boldsymbol{n} \cdot \mathcal{R} \cdot \boldsymbol{n} = We^{-1} K, \tag{2.6}$$

hold. Here $\mathcal{R}$ is the stress tensor, $We = \rho_0 RV^2/\sigma$ is the Weber number, σ is the surface tension coefficient, K is the free surface curvature and $\boldsymbol{n}$ and $\boldsymbol{t}$ are the unit vectors normal and tangential to the liquid surface, respectively. According to Stokes's law

$$\mathcal{R} = -pI + \frac{2}{Re}\left[\left(\frac{\partial \boldsymbol{u}}{\partial \boldsymbol{x}}\right) + \left(\frac{\partial \boldsymbol{u}}{\partial \boldsymbol{x}}\right)^*\right], \tag{2.7}$$

where I is the unit matrix, $(\partial \boldsymbol{u}/\partial \boldsymbol{x})$ is the Jacobian matrix and $(\partial \boldsymbol{u}/\partial \boldsymbol{x})^*$ is its conjugate. On the wetted part of the impacting rigid surface,

$$y = -Mt, \quad -a(t) < x < a(t), \tag{2.8}$$

and the no-slip conditions

$$v = -1, \tag{2.9}$$

$$u = 0, \tag{2.10}$$

have to be satisfied. The initial conditions for the impact problem are

$$\boldsymbol{u} = 0, \quad p = 0, \quad \rho = 1, \quad H(x, y, 0) = y + \tfrac{1}{2}M(x^2 + y^2), \quad a(0) = 0. \tag{2.11}$$

The flow is symmetrical with respect to the axis Oy in our case, therefore $u(x, y, t) = -u(-x, y, t)$, $v(x, y, t) = v(-x, y, t)$, $p(x, y, t) = p(-x, y, t)$, $H(-x, y, t) = H(x, y, t)$. In addition, the following conditions must also be satisfied: (A) the liquid particles cannot penetrate the rigid surface (2.8), i.e. $y \leqslant -Mt$ in (2.3); (B) the normal component of the stress vector $\boldsymbol{n} \cdot \mathcal{R} \cdot \boldsymbol{n}$ along the wetted region cannot be greater than a limiting value p_* which is dependent on the adhesive forces between the liquid and the solid in the region of their contact.

We will seek the solution of the problem (2.1)–(2.11) as $M \ll 1$, $Re \gg 1$, $We \gg 1$ and $Fr \gg 1$. The inequalities will be satisfied if the impact velocity V is such that

$$\max(\nu/R, \sqrt{\sigma/(\rho_0 R)}) \ll V \ll c_0.$$

This interval of the impact velocities can be achieved if

$$\max(\nu/c_0, \sigma/(\rho_0 c_0^2)) \ll R \ll c_0^2/g.$$

For example, this means 10^{-6} mm $\ll R \ll 2 \times 10^5$ m for impact on a water drop.

3. Acoustic solution

In the first four stages of the impact, when the dimensions of the disturbed flow region are comparable with the dimension of the contact spot, equations (2.3) and (2.4) and the initial conditions (2.11) provide

$$\rho = 1 + M\tilde{\rho}(x, y, t),$$
$$H(x, y, t) = y + M(\tfrac{1}{2}x^2 - h(x, y, t)), \tag{3.1}$$

$h(x, y, 0) = -\frac{1}{2}y^2$, for small Mach numbers. The transformation

$$y_1 = y + \tfrac{1}{2}M(x^2 + y^2), x_1 = x$$

maps the original position of the free surface close to the impact point, $x = O(1)$, $y = O(1)$, onto the line $y_1 = 0$. The position of the solid surface is now described by the equation

$$y_1 = M(\tfrac{1}{2}x^2 - t) + \tfrac{1}{2}M^2t^2, \tag{3.2}$$

and the position of the free surface by the equation

$$y_1 = Mh(x, y(x, y_1, t), t) + \tfrac{1}{2}M^3(\tfrac{1}{2}x^2 - h)^2. \tag{3.3}$$

It can be verified that this mapping does not change the equations of motion, or boundary or initial conditions at leading order when $M \to 0$. As a first step we assume that the unknown functions $\boldsymbol{u}$, p, $\tilde{\rho}$, h and all their derivatives appearing in (2.1)–(2.11) have bounded limits as $M \to 0$, $Re \to \infty$, $We \to \infty$, $Fr \to \infty$ and $t = O(1)$, $x = O(1)$, $y = O(1)$. In order to derive the boundary-value problem for the limiting values of the unknown functions, one can formally put $M = 0$, $Re^{-1} = 0$, $Fr^{-1} = 0$, $We^{-1} = 0$ in (2.1)–(3.3). At leading order the variables y and y_1 are identical, the flow is irrotational with the velocity potential $\phi(x, y, t)$ satisfying the wave equation

$$\phi_{tt} = \phi_{xx} + \phi_{yy} \tag{3.4}$$

in the lower half-plane $y < 0$, which is the image of a small vicinity of the contact region in the deformed coordinate system. The boundary conditions (2.4), (2.6) and (2.9) provide at leading order

$$h_t = \phi_y, \quad \phi_t = 0 \quad (y = 0, \quad |x| > a(t)), \tag{3.5}$$

$$\phi_y = -1 \quad (y = 0, \quad |x| < a(t)), \tag{3.6}$$

and the conditions (2.11) give

$$\phi = 0, \quad h = 0 \quad (y < 0, \quad t = 0). \tag{3.7}$$

It should be noted that the conditions (2.5) and (2.10) cannot be satisfied by the acoustic solution. The conditions (A) and (B) and equations (3.2) and (3.3) give

$$h(x, t) \leqslant \tfrac{1}{2}x^2 - t, \tag{3.8}$$

$$p \geqslant -p_*, \tag{3.9}$$

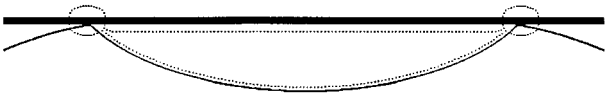

Figure 2. The flow pattern at the supersonic stage.

where $p = -\phi_t$ within the framework of the acoustic approximation (3.4)–(3.7).

Relations (3.4)–(3.9) form the acoustic model which is the basis of the study of liquid–solid impact at relatively low speeds, $V \ll c_0$. The acoustic model is analytical, but its study includes not only construction of the analytical solution, but also the analysis of this solution, with respect to its correspondence to the original equations (2.1)–(3.3) and the assumptions with lie at the heart of the acoustic approximation. It is worth noting that the problem (3.4)–(3.9) is the same as the problem of a blunt-body impact on the free surface of a weakly compressible liquid (Ogilvie 1963). The reason is that at the initial stage, which is under consideration here, it does not matter which surface—rigid or liquid—is curved near the point of the first contact.

If the shapes of the solid surface and the initial liquid surface are not as simple as those considered here, equation (3.2) for the shape of an equivalent entering body and the right-hand side of (3.8) have to be changed. The same technique can be used to derive the acoustic model of liquid–solid impact in the three-dimensional case. However, the three-dimensional model cannot be classified as being analytical, because its analysis is currently incomplete.

4. Supersonic stage

In the supersonic stage the free surface remains undisturbed and the dimension of the contact region can be determined from pure geometrical conditions (Lesser & Field 1983*a*). Equation (3.2) gives $a(t) = \sqrt{2t}$ in the leading order as $M \to 0$. This stage is over at the moment t_s, when $(\mathrm{d}a/\mathrm{d}t) = 1$. In dimensionless variables $t_s = 0.5$. The acoustic solution at the supersonic stage was first derived by Rochester (1979) for circular liquid drop impact. The generalization of the Rochester solution for an arbitrary geometry of the impact and the analysis of the acoustic solution was given by Korobkin (1992*b*). It was found that in the region of the disturbed flow (figure 2) this solution provides the approximate solution of the original problem (2.1)–(3.3) outside narrow zones close to: (i) the shock front; (ii) the rigid surface; and (iii) the contact points where the viscous effects are of importance. Inside each of these zones, inner asymptotic solutions have to be constructed and matched with the outer acoustic solution.

The flow inside the boundary layer on the rigid surface is viscous and linear. The thickness of the layer is of order $O(Re^{-1/2})$ as $Re \to \infty$. The shear stresses on the surface $p_{n\tau}$ are given as

$$p_{n\tau}(x,t) = \frac{2}{\sqrt{Re}}\left(\frac{x}{\sqrt{1-x^2}\sqrt{t-x^2/2}} - \int_{x^2/2}^{t} \frac{p_x(x,0,\tau)\,\mathrm{d}\tau}{\sqrt{t-\tau}}\right) H(\sqrt{2t}-|x|).$$

Here $p(x,0,t)$ is the acoustic pressure distribution along the rigid surface (see Rochester 1979) $p_x(x,0,t) \geqslant 0$, where $0 \leqslant x \leqslant \sqrt{2t}$. The stresses are zero at the centre of the contact region and are unbounded near the contact points. The flow near the shock front is linear, quasi-stationary and one dimensional to leading order as $Re \to \infty$. The problem of the viscous flow in this region is a classical one; it is well known as a problem of shock wave structure. The zones (i) and (ii) meet each

other at the contact points where both the inner solutions fail. In the vicinity of the right-hand contact point, $x = a(t)$, $y = -Mt$, it is convenient to introduce 'internal' variables λ, μ such that

$$x = a(t) + Re^{-1}\,\lambda, \quad y = -Mt + Re^{-1}\,\mu.$$

The flow in the vicinity is governed in the leading order by the equations

$$\dot{a}(t)\boldsymbol{u}_\lambda + \nabla p = \Delta\boldsymbol{u} + (\zeta/\eta + \tfrac{1}{3})\nabla(\nabla\cdot\boldsymbol{u}), \quad \dot{a}(t)p_\lambda + (\nabla\cdot\boldsymbol{u}) = 0 \quad (\mu < 0),$$

which follow from (2.1), (2.2). In the stretched variables we must put $Re = 1$ in (2.7), $We^{-1} = 0$ in (2.6), and $\boldsymbol{t} = (1, 0)$, $\boldsymbol{n} = (0, -1)$ in (2.5) and (2.6). The conditions (2.9), (2.10) remain the same but are now taken on the line $\mu = 0$, $\lambda < 0$. The conditions (2.5), (2.6) have to be satisfied on the line $\mu = 0$, $\lambda > 0$. The flow is quasi-stationary and linear. The boundary problem obtained can be reduced to the matrix factorization problem. The shear stresses in the vicinity are high, of order $O(\rho_0 c_0 V)$ in dimensional variables. Deformations of the free surface are localized near the contact points and decay exponentially with the distance. However, the flow pattern changes radically as $\dot{a} \to 1 + 0$.

The changes occur not only in the inner solution near the contact points but also in the outer (acoustic) solution. The supersonic stage is over and the transonic stage, where the speed of the contact region expansion is close to the local sound velocity, starts.

5. Transonic stage

The acoustic solution (see Korobkin 1992*b*) predicts that at the end of the supersonic stage, $t \to 0.5 - 0$, the liquid flow close to the contact points is approximately self-similar and is described by the formulae

$$u(x, y, t) = (0.5 - t)^{-1/2} U_* \left(\frac{x - a(t)}{(0.5 - t)^2}, \frac{y}{(0.5 - t)^{3/2}} \right) + \cdots,$$

$$v(x, y, t) = V_* \left(\frac{x - a(t)}{(0.5 - t)^2}, \frac{y}{(0.5 - t)^{3/2}} \right) + \cdots,$$

$$p(x, y, t) = u(x, y, t) + \cdots,$$

where U_*, V_* are bounded and continuous functions. The formulae indicate that the 'internal' variables and new unknown functions near the right-hand contact point have to be introduced as follows:

$$\left.\begin{array}{c} t = 0.5 + l\tau_1, \quad x = a(t) + l^2\lambda_1, \quad y_1 = l^{3/2}\mu_1, \\ u = l^{-1/2}U_1(\lambda_1, \mu_1, \tau_1), \quad p = l^{-1/2}p_1(\lambda_1, \mu_1, \tau_1), \quad v = V(\lambda_1, \mu_1, \tau_1). \end{array}\right\} \tag{5.1}$$

The small quantity l determines the duration of the stage. Substituting (5.1) into (2.1)–(2.4), (2.6), (2.8)–(3.3), where $Re^{-1} = 0$, $We^{-1} = 0$, $Fr^{-1} = 0$ and $M \ll 1$ means that the limiting relations as $M \to 0$ will contain the maximum possible number of terms if and only if $l = M^{2/3}$. The dimensional pressure p' therewith is of the order $O(\rho_0 c_0^{4/3} V^{2/3})$, in contrast to the acoustic pressure, which is of order $O(\rho_0 c_0 V)$. The duration of the transonic stage is of $O(M^{8/3}R/V)$. The viscous and capillary effects can be neglected if $Re \cdot M^{4/3} \gg 1$, $We \cdot M^{7/3} \gg 1$. For example, for the impact of a water drop with $R = 2$ mm and $V = 40$ m s^{-1}, we obtain $Re \cdot M^{4/3} \approx 6.5 \times 10^3$,

$We \cdot M^{7/3} \approx 10^3$. It is convenient to introduce new stretched variables (n is the constant in equation of state (2.3).

$$\tau_1 = \frac{1}{2k}(n+1)^{2/3}\tau, \quad \lambda_1 = \frac{1}{4k}(n+1)^{4/3}\lambda, \quad k = -\ddot{a}(t_s),$$

$$\mu_1 = \frac{1}{4k}(n+1)\mu, \quad p_1 = (n+1)^{-1/3}p, \quad U_1 = (n+1)^{-1/3}U,$$

with the help of which the initial boundary-value problem governing the flow near contact points can be written as

$$\frac{\partial U}{\partial \tau} + [U+\tau]\frac{\partial U}{\partial \lambda} + \frac{\partial V}{\partial \mu} = 0, \tag{5.2}$$

$$\frac{\partial U}{\partial \mu} = \frac{\partial V}{\partial \lambda}, \quad P = U \quad (\mu < 0, \quad \lambda < g(\mu,\tau)), \tag{5.3}$$

$$V = -1 \quad (\mu = 0, \quad \lambda < \lambda_c(\tau)), \tag{5.4}$$

$$\frac{\partial h}{\partial \lambda} = -V, \quad U = 0 \quad (\mu = 0, \quad \lambda_c(\tau) < \lambda < \lambda_s(\tau), \quad \tau > \tau_*), \tag{5.5}$$

$$V + \frac{\partial g}{\partial \mu}U = 0, \quad \frac{\partial g}{\partial \tau} - \left(\frac{\partial g}{\partial \mu}\right)^2 = \tfrac{1}{2}U + \tau \quad (\mu < 0, \quad \lambda < g(\mu,\tau)), \tag{5.6}$$

$$\lambda_s(\tau) = g(0,\tau), \tag{5.7}$$

$$\lambda_s(\tau) = \lambda_c(\tau) = 0 \quad (\tau < \tau_*), \tag{5.8}$$

$$\lambda_c(\tau) = \int_{\lambda_c(\tau)}^{\lambda_s(\tau)} V(\xi, 0, \tau)\,\mathrm{d}\xi \quad (\tau > \tau_*), \tag{5.9}$$

$$U \to 0 \quad (\tau \to -\infty). \tag{5.10}$$

Here the equations $\lambda = g(\mu,\tau)$ and $\mu = h(\lambda,\tau)$ describe the positions of the shock front and the free surface, respectively, $\lambda_c(\tau)$ is the distance between the contact point and the point of intersection of the solid surface with the undisturbed surface of the liquid volume (see figure 3). The unknown quantity τ_* is such that the shock front is attached to the contact point when $\tau < \tau_*$. Conditions (5.5) follow from the kinematic (2.4) and dynamic (2.6) conditions. Equations (5.8) mean that the free surface is undisturbed when $\tau < \tau_*$; (5.9) is the well-known Wagner condition. Condition (5.10) provides the matching of the outer acoustic solution with the inner transonic solution. The condition is very simple and makes it possible to study the flow at the transonic stage independently from the analysis of the outer solution. It is worth noting that the problem (5.2)–(5.10) differs from the acoustic model (3.4)–(3.7) by the additional term $U(\partial U/\partial\lambda)$ in (5.2) only. All other equalities are the same (conditions (5.6) on the shock front follow from the equations of motion (5.2), (5.3)). Equations (5.2), (5.3) show that there is a velocity potential $\Phi(\lambda,\mu,\tau)$, $U = P = \Phi_\lambda$, $V = \Phi_\mu$, which satisfies the equation

$$\Phi_{\lambda\tau} + (\tau + \Phi_\lambda)\Phi_{\lambda\lambda} + \Phi_{\mu\mu} = 0 \quad (\mu < 0).$$

The problem (5.2)–(5.10) does not contain any parameters and is the same for any geometry of the process and any equation of state. The derived transonic model is not able to describe the jet formation after the escape of the shock front onto the

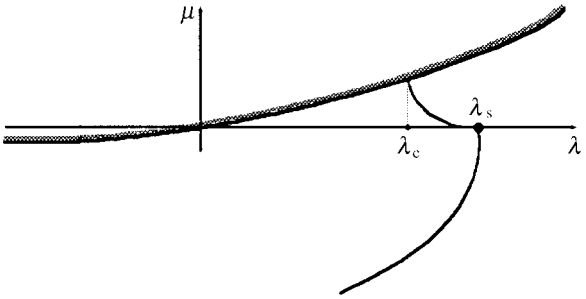

Figure 3. The flow pattern at the transonic stage near the right hand contact point.

free surface. Indeed, due to (5.5) the liquid particles of the free surface can move only vertically in this approximation.

The values of the unknown functions at the contact point, $\lambda = 0$, $\mu = 0$, when $\tau < \tau_*$ will be denoted by a subscript '0'. The conditions (5.4), (5.6) and (5.8) predict $U_0^3 + 2\tau U_0^2 + 2 = 0$. The solution of this cubic equation, which satisfies (5.10), is

$$U_0(\tau) = -\tfrac{8}{3}\tau \sin\tfrac{1}{6}\beta(\tau)\sin(\tfrac{1}{6}\beta(\tau) + \tfrac{1}{3}\pi), \quad \beta(\tau) = \cos^{-1}\left[1 + \left(\frac{3}{2\tau}\right)^3\right]$$

and exists up to the moment $\tau_* = -3 \cdot 2^{-4/3}$ ($\tau_* \approx -1.190\,55$), therewith $U_0(\tau_*) = 4^{1/3}$. This corresponds to the result given by Lesser (1981) as $M \to 0$.

The peculiarities of the flow are essentially dependent on the sign of the coefficient $U + \tau$ in (5.2). The coefficient is negative when $\tau < \tau_s$, where τ_s is the solution of the equation $U_0(\tau_s) + \tau_s = 0$. We find $\tau_s = -2^{1/3}$ ($\tau_s \approx -1.259\,921$). The solution of the problem (5.2)–(5.10) can be obtained as a Taylor series when $\tau < \tau_s$. In particular,

$$U_\lambda(0,0,\tau) = \frac{12U_0^5}{(4-U_0^3)(8-3U_0^3)}, \quad V_\mu(0,0,\tau) = -\frac{4U_0^3}{(4-U_0^3)(8-3U_0^3)},$$

$$g_{\mu\mu}(0,\tau) = -\frac{8U_0^2}{(4-U_0^3)(8-3U_0^3)}, \quad U_\mu(0,0,\tau) = 0, \quad V_\lambda(0,0,\tau) = 0,$$

$$\tau = -\frac{U_0^3+2}{2U_0^2}, \quad 0 < U_0 < 2^{1/3}.$$

It can be proved that the higher derivatives are the rational functions of U_0. Analytical expressions for the derivatives can be effectively obtained using computer algebra. At τ_s, a local subsonic zone appears near the contact point. The solution in the time interval $\tau_s < \tau < \tau_*$, $\tau_* - \tau_s < 0.07$, can be found only numerically. Analysis of the corresponding eigenvalue problem predicts that the solution is singular at the contact point

$$U = U_0(\tau) + O(r^{\alpha(\tau)}), \quad V = -1 + O(r^{\alpha(\tau)}), \quad g(\mu,\tau) = g_\mu^0(\tau)\mu + O(\mu^{1+\alpha(\tau)}),$$

$$\alpha(\tau) = \frac{\tan^{-1} C_2(\tau)}{\tan^{-1} C_1(\tau)}, \quad C_1(\tau) = U_0(\tau)\sqrt{U_0(\tau)+\tau},$$

$$C_2(\tau) = (4 - U_0^3(\tau))/(4U_0(\tau)\sqrt{U_0(\tau)+\tau}),$$

where $r = \sqrt{\lambda^2+\mu^2}$, $r \to 0$. It should be noted that $\alpha(\tau) \to 0$ as $\tau \to \tau_* - 0$. This means that the asymptotic expansions (5.1) are not uniformly valid at the end of

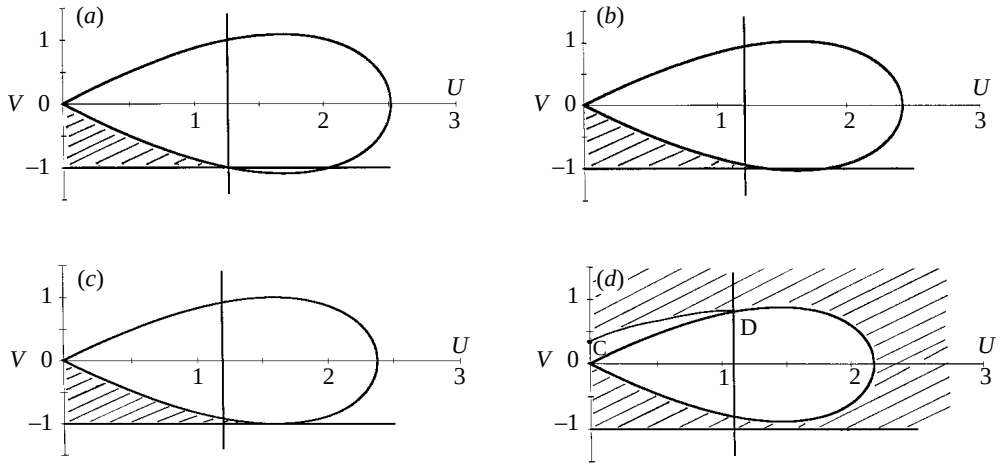

Figure 4. (*a*) Hodograph plane for the quasi-stationary approximation at $\tau = \tau_s$. The image of the flow region is shaded. (*b*) Hodograph plane for the quasi-stationary approximation at the moment when the pressure gradient becomes unbounded at the contact points. The image of the flow region is shaded. (*c*) Hodograph plane for the quasi-stationary approximation at $\tau = \tau_*$. The image of the flow region is shaded. (*d*) Hodograph plane for the quasi-stationary approximation at $\tau = \tau_* + 0.1$. The image of the flow region is shaded.

the regime with attached shock front and the viscous effects cannot be neglected. We expect that the model of viscous transonic flow (Sichel 1963) will give a realistic description of this phase.

In order to clarify the flow at $\tau > \tau_*$ the quasi-stationary approximation is used. Within the framework of this approach we drop all derivatives with respect to time in (5.2)–(5.10). The resulting problem is analysed by the hodograph method. The rigid surface, $\mu = 0$, $\lambda < 0$, corresponds to the line $V = -1$, and the free surface to the line $U = 0$, and the shock front to the curve $(\frac{1}{2}U + \tau)U^2 + V^2 = 0$ in the hodograph plane (figure 4). The last curve is referred to as the shock polar. The image of the flow region is shaded. Figure 4*d* shows that the structure of the flow changes at the moment τ_*. Here CD is the characteristic curve which corresponds to flow of Prandtl–Meyer type near the point where the shock front is attached to the free surface. This qualitative analysis is similar to that given by Guderley (1960) for supersonic flow around an infinite symmetrical wedge. The present analysis demonstrates that the deformation of the free surface near the contact points leads to a further increase in pressure when $\tau > \tau_*$. The pressure near the contact points will decrease only after a decrease in the speed of the contact spot expansion. Another very interesting feature of the flow after $\tau = \tau_*$ follows from figure 4*d*. It is seen that the pressure behind the shock front drops by a jump discontinuity after the front escapes onto the free surface. Correspondingly, the speed of the shock front will be reduced due to the relief wave coming from the free surface. At the same time, the contact point is accelerated due to the motion of the free surface towards the solid one. This means that disturbed part of the free surface grows after $\tau = \tau_*$ and then decays again. It is possible that this part will disappear and the shock front will again be attached to the contact points. This alalysis agrees with the numerical results of Pidsley (1983) and by Surov & Ageev (1989). The numerical analysis shows that the shock escape onto the free surface is an essentially non-stationary process with oscillations of the main flow characteristics. Nevertheless, the speed of the contact points will vanish

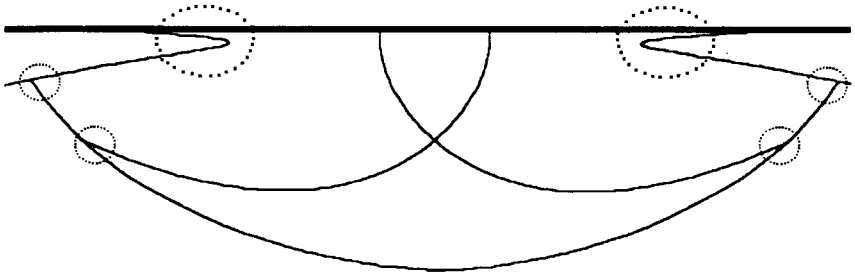

Figure 5. The flow pattern at the subsonic stage.

with time and at the end of the transonic stage the shock front will be far from the contact points. The deformations of the free surface will be small almost everywhere but the curvature of the free surface will be high in a small zone near the moving central points. It is expected that the nonlinear effects will be localized in this zone and can be approximately disregarded outside of it. The transonic stage is over and the subsonic stage starts.

6. Subsonic stage

The parts of the free surface which are involved in motion at this stage move towards the rigid surface additionally increasing its wetted area, $|x| < a(t)$, $y = -Mt$. The dimension of the contact region depends on the liquid flow and is unknown in advance. This is the main peculiarity of the subsonic stage. From the point of view of an analytical description of the impact process, the determination of the function $a(t)$ is a key problem. Only after the problem has been solved may we think about asymptotic analysis of the flow. It was found (Korobkin 1992*a*) that an approximate analytical formula for $a(t)$ could be derived within the framework of the acoustic approximation (3.4)–(3.7) with the help of condition (3.8). This result makes it possible to analyse the flow under the liquid–solid impact in all details. The wave pattern was found to be complicated but it is correctly predicted by the acoustic approach (Korobkin 1994*a*). Due to relief wave interaction, the pressure may drop below its atmospheric value close to the centre of the contact region, and interface cavitation may be observed (Brunton & Camus 1970; Brunton & Rochester 1979; Field *et al.* 1985). The possibility of the appearance of low pressure zones depends on the speed of the contact region expansion (Korobkin 1994*b*). The acoustic model provides the asymptotic solution of the original problem (2.1)–(2.11) inside the flow region but not near its boundary (figure 5). The boundary of the flow region can be divided into the following seven parts: (i) viscous boundary layer close to the central part of the shock front (see § 4); (ii) small vicinities of the points where the relief wave is attached to the shock front (the flow in this zone is two dimensional, nonlinear and is governed by the transonic approximation); (iii) zones of nonlinear interaction between the relief wave and the shock front (the flow is unsteady, one-dimensional to leading order, and nonlinear. Initial conditions can be derived from the solution at the transonic stage); (iv) small vicinities of the points where the shock front is attached to the free surface; (v) the viscous boundary layer along the free surface; (vi) the jet region; (vii) the viscous boundary layer along the wetted solid surface. The zones (ii), (iii), (iv) can be additionally divided into subzones to clarify the roles of viscous and acoustic effects. The flows inside these zones were analysed

by Berezin & Grib (1960) in connection with the problem of nonlinear reflection of plane shock at a free surface. A similar problem on impulsive wedge motion in a compressible liquid was studied by Titarenko (1981). Zone (vi) is divided into the jet root and jet region. The influence of the jet motion on the flow inside the jet root may be neglected. Respectively, the influence of the liquid motion inside the jet root on the flow in the main region may also be neglected in the first approximation. The dimensions of the jet root and the jet thickness are of order $O(M^3R)$ as $M \to 0$ in dimensional variables. The flow in the jet root is approximately quasi-stationary, nonlinear and essentially two-dimensional. The characteristics of the flow and the pressure distribution are given by the Chaplygin subsonic jet theory (Chaplygin 1904). In particular, the pressure along the solid surface inside the jet root is given by

$$p \sim \frac{2}{\sqrt{\pi}} \frac{\dot{a}^2}{V_0^2} \left(1 - \frac{\dot{a}^2}{c_0^2}\right)^{-1/4} h^{1/2} (a - x)^{-1/2},$$

as $M^{-2} \cdot (a - x) \to \infty$, i.e. far from the jet region. Here h is the jet thickness and $\dot{a}$ is the speed of the contact point. The formula agrees with that derived by Wagner (1932) for the incompressible liquid model when $\dot{a}/c_0 \to 0$. On the other hand, the acoustic theory predicts

$$p \sim \gamma_c(t)(a - x)^{-1/2} \tag{6.1}$$

close to the jet root; the coefficient $\gamma_c(t)$ is thereby known (Korobkin 1994*a*). Comparison of the pressures given by the Chaplygin theory and by the acoustic approximation (6.1) makes it possible to estimate the jet thickness h and other parameters of the jet flow. The liquid particles are accelerated inside the jet root up to velocities comparable with the sound speed. The particles which then come into the jet move at a velocity equal to twice that of the contact point, $2\dot{a}(t)$. These particles are not affected by any forces since the pressure inside the jet is close to atmospheric. This means that the particles in the jet move inertially. However, the capillary forces and the jet interaction with air become important with time and are responsible for the jet disintegration. That is why at the initial stage of jet formation, when the jet thickness is small, the jet observed in experiments (see Camus 1971) is very short and surrounded by a cloud of small drops. But with increasing time the jet thickness increases and the jet becames visible.

The speed of the contact region expansion drops with time as $O(t^{-1/2})$ but the speed of the shock propagation cannot be less than the sound velocity in the quiescent liquid. Therefore, the distance between the shock and the contact region grows with time. The acoustic effects decay close to the solid surface, being localized near the shock front. It is expected that the Wagner theory derived within the framework of the incompressible liquid model can be used to describe the flow near the contact region at the end of the subsonic stage, but the rate of convergence of the acoustic solution to the Wagner solution is quite small (Korobkin 1995). For example, the difference between the hydrodynamic forces predicted by the acoustic approximation and by the Wagner theory is of order $O(t^{-1/2})$ as $t \to \infty$. Nevertheless, the acoustic effects decay with time and their contribution becames much smaller than that of the inertia effects. The subsonic stage is over and the inertia stage starts.

7. Inertia stage

This stage was the subject of intensive study by Wagner (1932). It is worth noting that there is no time scale associated with this stage. It seems logically correct to consider this stage as the part of the subsonic stage when $t \gg 1$. The dimension of the contact region grows with time as $O(\sqrt{t})$, therefore, it is convenient to introduce new variables as follows:

$$x = x_1/\epsilon, \quad y = y_1/\epsilon, \quad t = t_1/\epsilon^2, \tag{7.1}$$

where ϵ is a formal small parameter, and consider the asymptotic behaviour of the combined solution at the subsonic stage as $\epsilon \to 0$. Correspondingly, the boundary problem, which describes the outer solution at the inertia stage, can be obtained by substituting (7.1) and $h = h_1/\epsilon^2$, $\phi = \phi_1/\epsilon$ into equations (3.4)–(3.9) and considerating their limits as $\epsilon \to 0$. We find that the left-hand side in (3.4) must be changed to zero and the initial conditions (3.7) have to be omitted. All other relations are the same as in the acoustic approximation. In order to construct a uniformly valid asymptotic solution close to the contact points, the jet solution in the jet root region is used (Wagner 1932; Armand & Cointe 1989; Howison *et al.* 1991).

It should be noted that there is no shock front in the Wagner scheme, because the distance between the shock and the contact region is of order $O(\epsilon^{-2})$ and is much greater than the length scale chosen. This leads to some contradictions of the Wagner theory when it is used without its connection with the general impact theory. The most famous contradiction is connected with the energy conservation law which does not hold within the framework of the Wagner approach (see Korobkin 1996). The first attempt to incorporate the acoustic effects into the impact theory was made by Grigoryan (1962). He considered the nonlinear self-similar problem of symmetrical wedge penetration into a weakly compressible liquid. It was shown that near the entering body the nonlinear model of the ideal incompressible liquid can be used, but far from the body the acoustic model provides the correct description of the flow.

These reasonings demonstrate that the acoustic effects will be localized near the shock front for large times. The analysis of the shock propagation through the liquid bulk and the shock interaction with the liquid boundaries are important in connection with the shock reflection at the rear side of the drop and possible subsequent cavitation inside the liquid (Camus 1971). In order to describe the flow far from the impact region, the following new variables are introduced:

$$x = x_2/\epsilon^2, \quad y = y_2/\epsilon^2, \quad t = t_2/\epsilon^2, \tag{7.2}$$

where $\epsilon \ll 1$, $\epsilon = O(M^{1/2})$ as $M \to 0$ and $x_2 = O(1)$, $y_2 = O(1)$, $t_2 = O(1)$. If $\epsilon^{-1}M^{1/2} \to 0$ as $M \to 0$, the acoustic model provides the approximate solution for large times. In particular, the pressure distribution far from the contact region is

$$p(x, y, t) \sim -\frac{y}{\pi\hat{r}} \int_1^{t/\hat{r}} F'(t - \hat{r}\alpha) \frac{\alpha \, \mathrm{d}\alpha}{\sqrt{\alpha^2 - 1}} \tag{7.3}$$

as $\hat{r} \to \infty$ and $t \to \infty$, where $\hat{r} = (x^2 + y^2)^{1/2}$ and $F(t)$ is the hydrodynamic force on the rigid moving surface. At the supersonic stage the force is equal to the product of one-dimensional impact pressure, which is unity in the non-dimensional variables, and the wetted area, which is $2\sqrt{2t}$ in our case (see Skalak & Feit 1966). Thus, $F(t) = 2\sqrt{2t}$ when $0 < t < \frac{1}{2}$. There is no formula available for $F(t)$ when $t > \frac{1}{2}$, but from the Wagner theory we know that $F(t) \to 2\pi$ as $t \to \infty$. The rate of convergence is expected to be very low: $F(t) - 2\pi = O(t^{-1/2})$ as $t \to \infty$ (Korobkin 1995).

It is worth noting that the function on the right-hand side of (7.3) is the exact solution of the problem (3.4)–(3.7) where the boundary conditions are changed to $p = F(t)\delta(x)$, $\delta(x)$ is the Dirac delta-function. The asymptotic formula (7.3) is derived by the averaging procedure and takes into account that the distances between the shock front and the relief waves are small. The pressure along the shock front, $t/\hat{r} \to 1 + 0$, is given as

$$p \sim \sin\varphi/\sqrt{\hat{r}},$$

where $\sin\varphi = -y/\hat{r}$, and does not correspond to the distribution provided by the classical geometrical acoustic.

If $\epsilon = \sqrt{M}$ the length scale will be equal to R for the new variables, and the time scale will be R/c_0. The last quantity is equal to the time the acoustic front takes to reach the drop centre. The deformation of the drop is estimated as $O(MR)$ and can be neglected at the time interval under consideration. As the result, we obtain the acoustic model which governes the liquid flow inside the drop at the inertia stage far from the contact region (see Lesser & Field 1983*b*). Within the framework of this model the pressure distribution is given by the function $q(x_2, y_2, t_2)$, $p = \sqrt{M}q$, which satisfies the wave equation

$$\frac{\partial^2 q}{\partial t_2^2} = \frac{\partial^2 q}{\partial r^2} + \frac{1}{r}\frac{\partial q}{\partial r} + \frac{1}{r^2}\frac{\partial^2 q}{\partial \theta^2} \tag{7.4}$$

inside the circle $r \leqslant 1$, where $x_2 = r\sin\theta$, $y_2 = 1 - r\cos\theta$, is equal to zero outside the contact region, and has to correspond to the asymptotic formula (7.3) close to the impact region. It is worth noting that the last matching condition is equivalent to the boundary condition

$$q = \sqrt{M}F(t_2/M)\delta(\theta) \quad (r = 1). \tag{7.5}$$

The scale of the acoustic pressure p is equal to $\rho_0 c_0^{1/2} V^{3/2}$. The dimension of the contact region is of order $O(\sqrt{M}t_2)$ and tends to zero as $M \to 0$.

The flow inside the drop at leading order does not influence the pressure distribution close to the contact region when $0 < t_2 < 4$. Therefore, the dimension of the contact region and the pressure distribution along it are determined by the acoustic approximation (3.4)–(3.7) when $t_2 = O(M)$ and by the Wagner theory when $t_2 < 4$. This means that the model (7.4), (7.5), with the initial conditions

$$q = 0, \quad \frac{\partial q}{\partial t_2} = 0 \quad t_2 = 0, \quad r < 1, \tag{7.6}$$

is valid when $0 < t_2 < 4$. With the help of the response function $\hat{q}(r, \theta, t_2)$, which satisfies (7.4)–(7.6) and the boundary condition $\hat{q}(1, \theta, t_2) = \delta(\theta)$ when $t_2 > 0$, the solution can be written as

$$q(r, \theta, t_2) = M^{-1/2} \int_0^{t_2} F'(\tau/M)\hat{q}(r, \theta, t_2 - \tau)\,\mathrm{d}\tau.$$

The dimension of the narrow zone where the acoustic effects are of major importance at the inertia stage can be estimated as $O(M)$ for small Mach numbers. This is why we can use geometrical acoustic theory to estimate the intensity of relief waves and to analyse the wave pattern as suggested by Lesser & Field (1983*b*). In this theory signals propagate along the rays with the origin at the point $x_2 = 0$, $y_2 = 0$. Close to the origin, the signal intensities have to correspond to the acoustic solution

(7.3). The calculations predict that the focusing of the relief waves coming from the rear side of the circular drop occurs at the symmetry axis at the distance $\frac{2}{3}R$ from the drop top. The experimental results by Camus (1971) and Field *et al.* (1989) give distances in the ranges $0.5R \div 0.62R$ and $0.5R \div 0.72R$, respectively, which roughly correspond to the theoretical estimation. The geometrical acoustic theory does not give any details of the pressure distribution behind the wave fronts, which can be very complicated. That is why the careful analysis of the problem based on the model (7.4)–(7.6) is very desirable.

8. Conclusion

It was shown in the present paper that the asymptotic approach to the impact problem clarifies the roles of different impact models and demonstrates the links between them, as well as the areas of the model validities. At the same time this approach provides new ideas to design experiments on impact and to derive adequate numerical algorithms to treat the impact problems. The idea to divide difficulties and to analyse them separately is very attractive and with careful realization, would lead to progress in the study of liquid–solid impact.

The paper was prepared for publication during the author's stay at the Department of Naval Architechture and Ocean Engineering, Hydrodynamics Laboratory, University of Glasgow. The author thanks the Royal Society for their support of this visit and Professor J. E. Field and Professor D. H. Peregrine for reading and correcting this paper.

References

Armand, J. L. & Cointe, R. 1986 Hydrodynamic impact analysis of a cylinder. In *Proc. Fifth Int. Offshore Mech. and Arctic Engng. Symp. (OMAE), Tokyo, Japan.* vol. 1, pp. 609–634. New York: ASME.

Berezin, O. A. & Grib, A. A. 1960 Non-regular reflection of plane shock at liquid free surface. *Zh. Prikl. Mekh. Tekh. Fiz.* **2**, 34–39.

Bowden, F. P.& Field, J. E. 1964 The brittle fracture of solids by liquid impact, by solid impact, and by shock. *Proc. R. Soc. Lond.* A **282**, 331–352.

Brunton, J. H. & Camus, J.-J. 1970 Flow in cavitation and drop impact studies. In *Proc. 9th Int. Conf on High-Speed Photography* (ed. W. G. Hyzer & W. G. Chase), pp. 444–450. New York: SMPTE.

Brunton, J. H. & Rochester, M. C. 1979 Erosion of solid surfaces by the impact of liquid drops. In *Erosion* (ed. C. H. Preece), pp. 185–248. New York: Academic.

Camus, J.-J. 1971 Ph.D. thesis, University of Cambridge.

Chaplygin, S. A. 1904 On gas jets. *Sci. Ann. Imp. Univ. Moscow, Phys.-Math. Div.* **21** (or NACA TM1063), 1–121.

Field, J. E., Lesser, M. B. & Dear, J. P. 1985 Studies of two-dimensional liquid-wedge impact and their relevance to liquid drop impact problems. *Proc. R. Soc. Lond.* A **401**, 225–249.

Field, J. E., Dear, J. P. & Ögren, J.-E. 1989 *J. Appl. Phys.* **65**, 533.

Grigoryan, S. S. 1962 On the work of Z. N. Dobrovol'skaya 'Penetration of a wedge into a compressible half-space'. *Prikl. Mat. Mech.* **26**, 557–558.

Guderley, K. G. 1960 *The theory of transonic flow.* Int. Series of Monographs in Aeronautics and Astronautics. New York: Pergamon.

Howison, S. D., Ockendon, J. R. & Wilson, S. K. 1991 Incompressible water-entry problems at small deadrise angles. *J. Fluid Mech.* **222**, 215–230.

Korobkin, A. A. 1992*a* Acoustic approximation in the problem of penetration of a blunt contour into ideal fluid. *Zh. Prikl. Mekh. Tekh. Fiz.* **4**, 48–54.

Korobkin, A. A. 1992*b* Blunt-body impact on a compressible liquid surface. *J. Fluid Mech.* **244**, 437–453.

Korobkin, A. A. 1994*a* Blunt-body impact on the free surface of a compressible liquid. *J. Fluid Mech.* **263**, 319–342.

Korobkin, A. A. 1994*b* Low-pressure zones under a liquid–solid impact. In *Proc. IUTAM Symposium on Bubble Dynamics and Interface Phenomena* (ed. J. R. Blake & N. H. Thomas), pp. 375–381. Dordrecht: Kluwer.

Korobkin, A. A. 1995 Acoustic effects on water impact. In *10th Workshop on Water Waves and Floating Bodies, Oxford*.

Korobkin, A. A. 1996 Global characteristics of jet impact. *J. Fluid Mech.* **307**, 63–84.

Lesser, M. B. 1981 Analytic solutions of liquid-drop impact problems. *Proc. R. Soc. Lond.* A **377**, 289–308.

Lesser, M. B. & Field, J. E. 1983*a* The impact of compressible liquids. *Ann. Rev. Fluid Mech.* **15**, 97–122.

Lesser, M. B. & Field, J. E. 1983*b* The geometric wave theory of liquid impact. *Proc. 6th Int. Conf. on Erosion by Liquid and Solid Impact*, pp. 17(1)–17(9). Cambridge.

Ogilvie, T. F. 1963 Compressibility effects in ship slamming. *Schffstechnik* **10**, 147–154.

Pidsley, P. H. 1983 A numerical investigation of water drop impact. In *Proc. 6th Int. Conf. on Erosion by Liquid and Solid Impact*, pp. 18(1)–18(6). Cambridge.

Rochester, M. C. 1979 The impact of a liquid drop and the effect of liquid properties on erosion. Ph.D. thesis, University of Cambridge.

Sichel, M. 1963 Structure of weak non-Hugoniot shocks. *Phys. Fluids* **6**, 653–662.

Skalak, R. & Feit, D. 1966 Impact on the surface of a compressible fluid. *Trans. ASME, J. Engng Ind.* **88B**, 325–331.

Surov, V. S. & Ageev, S. G. 1989 Two-dimensional simulation of collision of compressible liquid drops with a target. *Izv. SO AN SSSR, Ser. Tekh. Nauk* **4**, 66–71.

Titarenko, V. V. 1981 On the problem of impulsive wedge motion. *Zh. Prikl. Mekh. Tekh. Fiz.* **4**, 155–165; 34–39. (In Russian.)

Van Dyke, M. 1964 *Perturbation methods in fluid mechanics.* New York: Academic.

Wagner, H. 1932 Uber Stoss- und Gleitvorgange an der Oberflache von Flussigkeiten. *Z. Angew. Math. Mech.* **12**, 193–215.